

¹ The human visual system preserves the hierarchy
² of 2-dimensional pattern regularity

³ Peter J. Kohler^{1,2,3} and Alasdair D. F. Clarke⁴

⁴ *¹ York University, Department of Psychology, Toronto, ON M3J 1P3, Canada*

⁵ *² Centre for Vision Research, York University, Toronto, ON, M3J 1P3, Canada*

⁶ *³Stanford University, Department of Psychology, Stanford, CA 94305, United States*

⁷ *⁴University of Essex, Department of Psychology, Colchester, UK, CO4 3SQ*

⁸ **Abstract**

Symmetries are present at many scales in images of natural scenes. A large body of literature has demonstrated contributions of symmetry to numerous domains of visual perception. The four fundamental symmetries, reflection, rotation, translation and glide reflection, can be combined in exactly 17 distinct ways. These *wallpaper groups* represent the complete set of symmetries in 2D images and have recently found use in the vision science community as an ideal stimulus set for studying the perception of symmetries in textures. The goal of the current study is to provide a more comprehensive description of responses to symmetry in the human visual system, by collecting both brain imaging (Steady-State Visual Evoked Potentials measured using high-density EEG) and behavioral (symmetry detection thresholds) data using the entire set of wallpaper groups. This allows us to probe the hierarchy of complexity among wallpaper groups, in which simpler groups are subgroups of more complex ones. We find that this hierarchy is preserved almost perfectly in both behavior and brain activity: A multi-level Bayesian GLM indicates that for most of the 63 subgroup relationships, subgroups produce lower amplitude responses in visual cortex (posterior probability: > 0.95 for 56 of 63) and require longer presentation durations to be reliably detected (posterior probability: > 0.95 for 49 of 63). This systematic pattern is seen only in visual cortex and only in components of the brain response known to be symmetric-specific. Our results show that representations of symmetries in the human brain are precise and rich in detail, and that this precision is reflected in behavior. These findings expand our understanding of symmetry perception, and open up new avenues for research on how fine-grained representations of regular textures contribute to natural vision.

Symmetries are abundant in natural and man-made environments, due to a complex interplay of physical forces that govern pattern formation in nature. Symmetrical patterns have been created and appreciated by human cultures throughout history and since the gestalt movement of the early 20th century, symmetry has been recognized as important for visual perception. Symmetry contributes to the perception of shapes (Palmer, 1985; Li et al., 2013), scenes (Apthorp and Bell, 2015) and surface properties (Cohen and Zaidi, 2013), as well as the social process of mate selection (Møller, 1992). Most of this work has focused on mirror symmetry or *reflection*, with much less attention being paid to the other fundamental symmetries: *rotation*, *translation*

38 and *glide reflection*. In the two spatial dimensions relevant for images, these four symmetries can
39 be combined in 17 distinct ways, *the wallpaper groups* (Fedorov, 1891; Polya, 1924; Liu et al., 2010).
40 Previous work on a subset of four of the wallpaper groups used functional MRI to demonstrate
41 that rotation symmetries in wallpapers elicit parametric responses in several areas in occipital
42 cortex, beginning with visual area V3 (Kohler et al., 2016). This effect was also robust with
43 electroencephalography (EEG), whether measured using Steady-State Visual Evoked Potentials
44 (SSVEPs) (Kohler et al., 2016) or event-related paradigms (Kohler et al., 2018). Here we extend this
45 work by collecting SSVEPs and psychophysical data from human participants viewing the full set
46 of wallpaper groups. We measure responses in visual cortex to 16 out of the 17 wallpaper groups,
47 with the 17th serving as a control stimulus. Our goal is to provide a more complete picture of
48 how wallpaper groups are represented in the human visual system.

49 A wallpaper group is a topologically discrete group of isometries of the Euclidean plane, i.e.
50 transformations that preserve distance (Liu et al., 2010). Wallpaper groups differ in the number
51 and kind of these transformations and we can uniquely refer to different groups using crystallo-
52 graphic notation. Full details of this naming convention can be found XXXX, but in brief, most
53 groups have are notated by pXZ , where $X \in \{1, 2, 3, 4, 6\}$ indicates the highest order of rotational
54 symmetry and $Z \in \{m, g\}$ indicates whether the pattern contains *mirror* or *glide* symmetry. See
55 Figure XXX for examples.

56 In mathematical group theory, when the elements of one group is completely contained in
57 another, the inner group is called a subgroup of the outer group (Liu et al., 2010). The full list
58 of subgroup relationships is listed in Section 1.4.2 of the Supplementary Material. Subgroup
59 relationships between wallpaper groups can be distinguished by their indices. The index of a
60 subgroup relationship is the number of cosets, i.e. the number of times the subgroup is found in
61 the supergroup (Liu et al., 2010). As an example, let us consider groups P_2 and P_6 . If we ignore
62 the translations in two directions that both groups share, group P_6 consists of the set of rotations
63 $\{0^\circ, 60^\circ, 120^\circ, 180^\circ, 240^\circ, 300^\circ\}$, in which $P_2 \{0^\circ, 180^\circ\}$ is contained. P_2 is thus a subgroup of P_6 ,
64 and P_6 can be generated by combining P_2 with rotations $\{0^\circ, 120^\circ, 240^\circ\}$. Because P_2 is repeated
65 three times in P_6 , P_2 is a subgroup of P_6 with index 3 (Liu et al., 2010). The 17 wallpaper groups
66 thus obey a hierarchy of complexity where simpler groups are subgroups of more complex ones
67 (Coxeter and Moser, 1972).

68 The two datasets we present here make it possible to assess the extent to which both behavior
69 and brain responses follow the hierarchy of complexity expressed by the subgroup relationships.
70 Based on previous brain imaging work showing that patterns with more axes of symmetry pro-
71 duce greater activity in visual cortex (Sasaki et al., 2005; Kohler et al., 2018, 2016; Keefe et al., 2018),
72 we hypothesized that more complex groups would produce larger SSVEPs. For the psychophys-
73 ical data, we hypothesized that more complex groups would lead to shorter symmetry detection
74 thresholds, based on previous data showing that under a fixed presentation time, discriminability
75 increases with the number of symmetry axes in the pattern (Wagemans et al., 1991). Our results
76 confirm both hypotheses, and show that activity in human visual cortex is remarkably consistent
77 with the hierarchical relationships between the wallpaper groups, with SSVEP amplitudes and
78 psychophysical thresholds following these relationships at a level that is far beyond chance. The

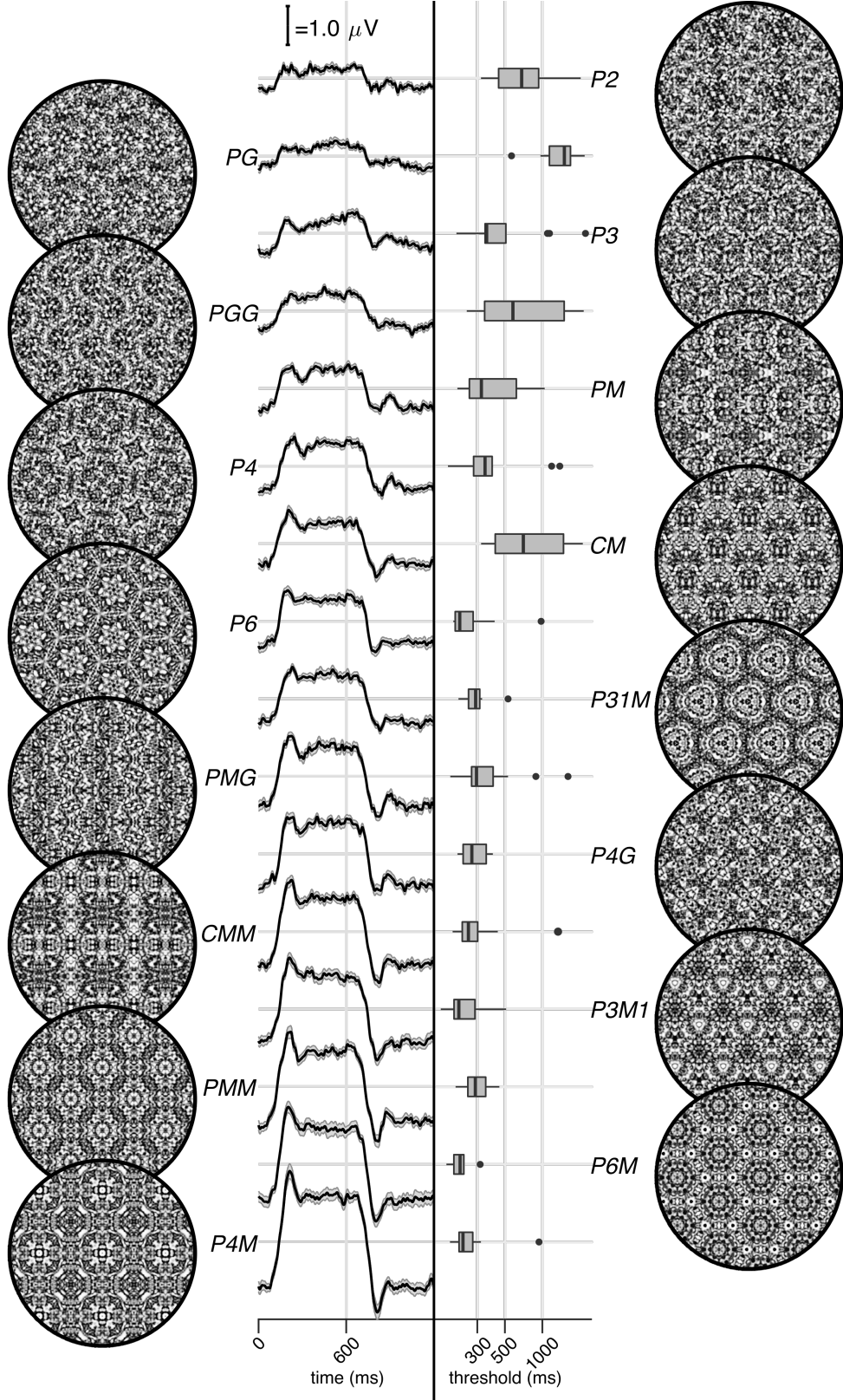


Figure 1: Examples of each of the 16 wallpaper groups are shown in the left- and right-most column of the figures, next to the corresponding SSVEP (center-left) and psychological (center-right) data from each group. The SSVEP data are odd-harmonic-filtered cycle-average waveforms. In each cycle, a P_1 exemplar was shown for the first 600 ms, followed by the original exemplar for the last 600 ms. Errorbars are standard error of the mean. Psychophysical data are presented as boxplots reflecting the distribution of display duration thresholds. The 16 groups are ordered by the strength of the SSVEP response, to highlight the range of response amplitudes.

79 human visual system thus appears to encode all of the fundamental symmetries using a represen-
80 tational structure that closely approximates the subgroup relationships from group theory.

81 Results

82 The stimuli used in our two experiments were generated from random-noise textures, which
83 made it possible to generate multiple exemplars from each of the wallpaper groups, as described
84 in detail elsewhere (Kohler et al., 2016). We generated control stimuli matched to each exemplar
85 in the main stimulus set, by scrambling the phase but maintaining the power spectrum. All
86 wallpaper groups are inherently periodic because of their repeating lattice structure. Phase
87 scrambling maintains this periodicity, so the phase-scrambled control images all belong to group
88 P_1 regardless of group membership of the original exemplar. P_1 contains no symmetries other
89 than translation, while all other groups contain translation in combination with one or more of the
90 other three fundamental symmetries (reflection, rotation, glide reflection) (Liu et al., 2010). In our
91 SSVEP experiment, this stimulus set allowed us to isolate brain activity specific to the symmetry
92 structure in the exemplar images from activity associated with modulation of low-level features,
93 by alternating exemplar images and control exemplars. In this design, responses to structural
94 features beyond the shared power spectrum, including any symmetries other than translation,
95 are isolated in the odd harmonics of the image update frequency (Kohler et al., 2016; Norcia et al.,
96 2015, 2002). Thus, the combined magnitude of the odd harmonic response components can be
97 used as a measure of the overall strength of the visual cortex response.

98 The psychophysical experiment took a distinct but related approach. In each trial an exemplar
99 image was shown with its matched control, one image after the other, and the order varied pseudo-
100 randomly such that in half the trials the original exemplar was shown first, and in the other half
101 the control image was shown first. After each trial, participants were instructed to indicate
102 whether the first or second image contained more structure. The duration of both images was
103 controlled by a staircase procedure so that a threshold duration for symmetry detection could be
104 computed for each wallpaper group.

105 Examples of the wallpaper groups and a summary of our brain imaging and psychophysical
106 measurements are shown in Figure 1. For our primary SSVEP analysis, we only considered EEG
107 data from a pre-determined region-of-interest (ROI) consisting of six electrodes over occipital cor-
108 tex (see Supplementary Figure 1.1). SSVEP data from this ROI was filtered so that only the odd
109 harmonics that capture the symmetry response contribute to the waveforms. While waveform am-
110 plitude is quite variable among the 16 groups, all groups have a sustained negative-going response
111 that begins at about the same time for all groups, 180 ms after the transition from the P_1 control
112 exemplar to the original exemplar. To reduce the amplitude of the symmetry-specific response to
113 a single number that could be used in further analyses and compared to the psychophysical data,
114 we computed the root-mean-square (RMS) over the odd-harmonic-filtered waveforms. The data
115 in Figure 1 are shown in descending order according to RMS. The psychophysical results, shown
116 in box plots in Figure 1, were also quite variable between groups, and there seems to be a general
117 pattern where wallpaper groups near the top of the figure, that have lower SSVEP amplitudes,

118 also have longer psychophysical threshold durations.

119 We now wanted to test our two hypotheses about how SSVEP amplitudes and threshold du-
120 rations would follow subgroup relationships, and thereby quantify the degree to which our two
121 measurements were consistent with the group theoretical hierarchy of complexity. We tested
122 each hypothesis using the same approach. We first fitted a Bayesian model with wallpaper group
123 as a factor and participant as a random effect. We fit the model separately for SSVEP RMS and
124 psychophysical data and then computed posterior distributions for the difference between su-
125 pergroup and subgroup. These difference distributions allowed us to compute the conditional
126 probability that the supergroup would produce (a) larger RMS and (b) a shorter threshold dura-
127 tions, when compared to the subgroup. The posterior distributions are shown in Figure 2 for
128 the SSVEP data, and in Figure 3 for the psychophysical data, which distributions color-coded
129 according to conditional probability. For both data sets our hypothesis is confirmed: For the
130 overwhelming majority of the 63 subgroup relationships, supergroups are more likely to produce
131 larger symmetry-specific SSVEPs and shorter symmetry detection threshold durations, and in
132 most cases the conditional probability of this happening is extremely high.

133 We also ran a control analysis using (1) odd-harmonic SSVEP data from a six-electrode ROI
134 over parietal cortex (see Supplementary Figure 1.1) and (2) even-harmonic SSVEP data from the
135 same occipital ROI that was used in our primary analysis. By comparing these two control
136 analysis to our primary SSVEP analysis, we can address the specify of our effects in terms of
137 location (occipital cortex vs parietal cortex) and harmonic (odd vs even). For both control analyses
138 (plotted in Supplementary Figures 3.3 and 3.4), the correspondence between data and subgroup
139 relationships was substantially weaker than in the primary analysis. We can quantify the strength
140 of the association between the data and the subgroup relationships, by asking what proportion of
141 subgroup relationships that reach or exceed a range of probability thresholds. This is plotted in
142 Figure 4, for our psychophysical data, our primary SSVEP analysis and our two control SSVEP
143 analyses. It shows that odd-harmonic SSVEP data from the occipital ROI and symmetry detection
144 threshold durations both have a strong association with the subgroup relationships such that a
145 clear majority of the subgroups survive even at the highest threshold we consider ($p(\Delta > 0 | data) >$
146 0.99). The association is far weaker for the two control analyses.

147 SSVEP data from four of the wallpaper groups (P_2 , P_3 , P_4 and P_6) was previously published
148 as part of our earlier demonstration of parametric responses to rotation symmetry in wallpaper
149 groups(Kohler et al., 2016). We replicate that result using our Bayesian approach, and find an
150 analogous parametric effect in the psychophysical data (see Supplementary Figure 4.1). We also
151 conducted an analysis testing for an effect of index in our two datasets and found that subgroup
152 relationships with higher indices tended to produce greater pairwise differences between the
153 subgroup and supergroup, for both SSVEP RMS and symmetry detection thresholds (see Supple-
154 mentary Figure 4.2). The effect of index is relatively weak, but the fact that there is a measurable
155 index effect can nonetheless be taken as preliminary evidence that representations of symmetries
156 in wallpaper groups may be compositional.

157 Finally, we conducted a correlation analysis comparing SSVEP and psychophysical data and
158 found a reliable correlation ($R^2 = 0.44$, Bayesian confidence interval [0.28, 0.55]). The correlation

reflects an inverse relationship: For subgroup relationships where the supergroup produces a much *larger* SSVEP amplitude than the subgroup, the supergroup also tends to produce a much *smaller* symmetry detection threshold. This is consistent with our hypotheses about how the two measurements relate to symmetry representations in the brain, and suggests that our brain imaging and psychophysical measurements are at least to some extent tapping into the same underlying mechanisms.

Discussion

Here we show that beyond merely responding to the elementary symmetry operations of reflection (Sasaki et al., 2005) and rotation (Kohler et al., 2016), the visual system represents the hierarchical structure of the 17 wallpaper groups, and thus every composition of the four fundamental symmetries (rotation, reflection, translation, glide reflection) which comprise the set of regular textures. Both SSVEP amplitudes and symmetry detection thresholds preserve the hierarchy of complexity among the wallpaper groups that is captured by the subgroup relationships (Coxeter and Moser, 1972). For the SSVEP, this remarkable consistency was specific to the odd harmonics of the stimulus frequency that are known to capture the symmetry-specific response (Kohler et al., 2016) and to electrodes in a region-of-interest (ROI) over occipital cortex. When the same analysis was done using the odd harmonics from electrodes over parietal cortex (Supplementary Figure 3.3) or even harmonics from electrodes over occipital cortex (Supplementary Figure 3.4), the data was substantially less consistent with the subgroup relationships (yellow and green lines, Figure 4).

The current data provide a description of the visual system's response to the complete set of symmetries in the two-dimensional plane. Our design precludes us from independently measure the response to P_1 , but because each of the 16 other groups produce non-zero odd harmonic amplitudes (see Figure 1), we can conclude that the relationships between P_1 and all other groups, where P_1 is the subgroup, are also preserved by the visual system. The subgroup relationships are in many cases not obvious perceptually, and most participants had no knowledge of group theory. Thus, the visual system's ability to preserve the subgroup hierarchy does not depend on explicit knowledge of the relationships. Previous behavioral experiments have shown that although naïve observers can distinguish many of the wallpaper groups (Landwehr, 2009), they tend to sort them into fewer groups than there actually are (4-12 groups) and it is common for exemplars from different wallpaper groups to be sorted in the same group (Clarke et al., 2011). The more controlled two-interval forced choice approach used in the current behavioral experiment allows us to show that more granular representations of wallpaper groups are measurable in behavior.

We observe a reliable correlation between our brain imaging and psychophysical data. This suggests that the two measurements reflect the same underlying symmetry representations in visual cortex. While it should be noted that the correlation is relatively modest ($R^2 = 0.44$), we note that this may be partly due to the fact that the same individuals did not participate in the two experiments. Future work in which behavioral and brain imaging data are collected from the

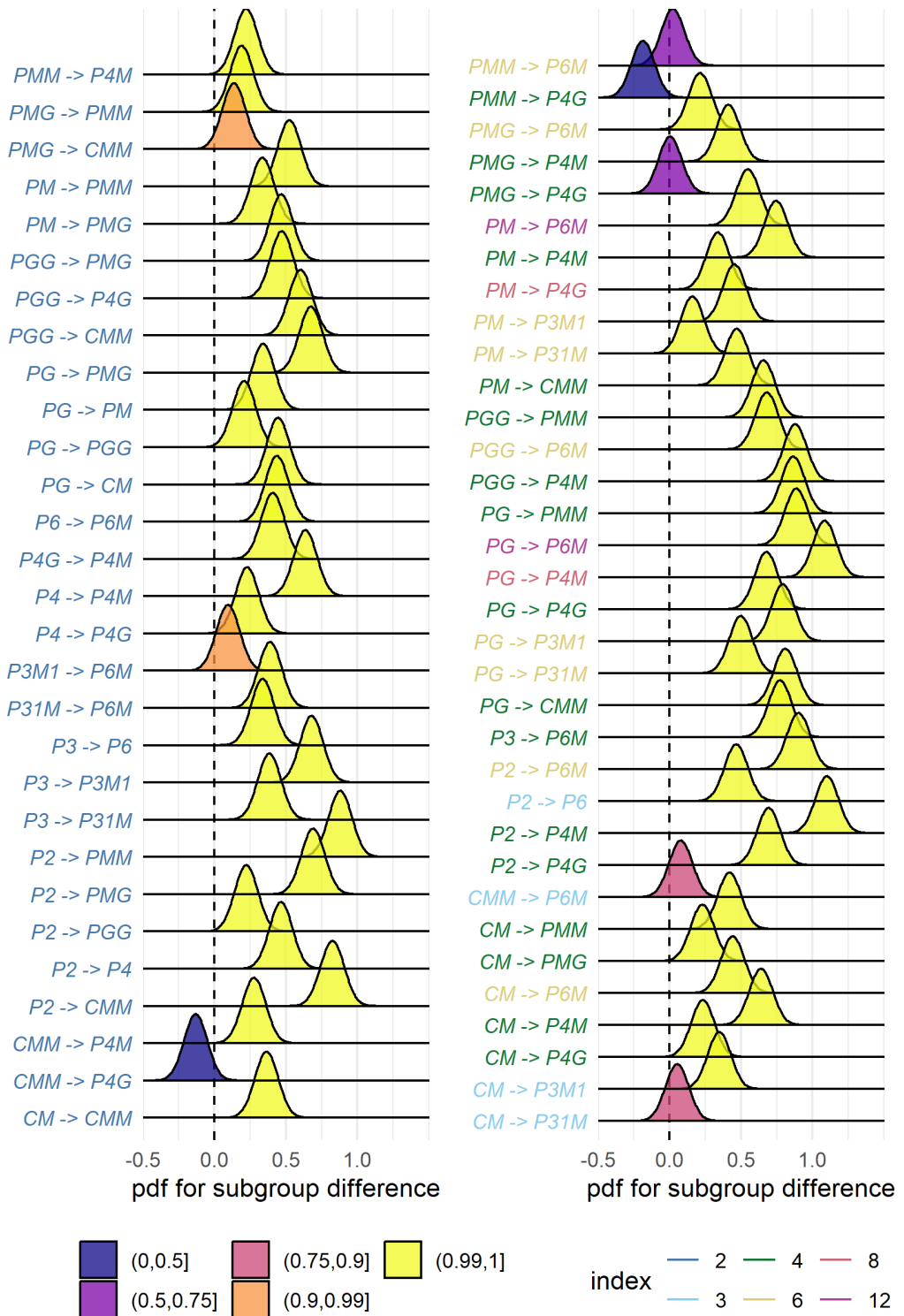


Figure 2: Posterior distributions for the difference in mean SSVEP RMS amplitude. Colour coding of the text indicates the index of the subgroup, while the colour of the filled distribution relates to the conditional probability that the difference in means is greater than zero. We can see that 55/63 subgroup relationships have $p(\Delta|data) > 0.99$.

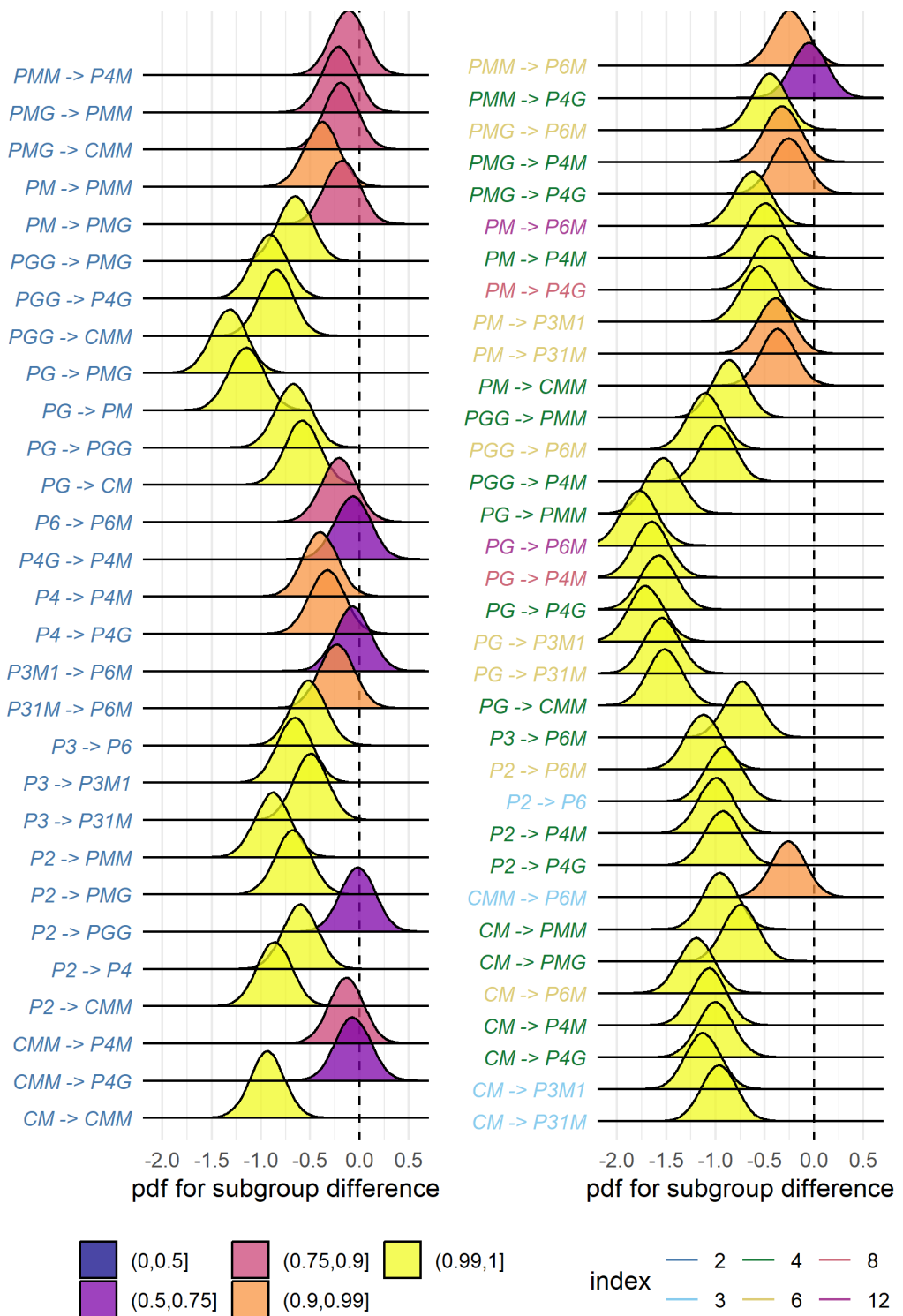


Figure 3: Posterior distributions for the difference in mean symmetry detection threshold durations. Colour coding of the text indicates the index of the subgroup, while the colour of the filled distribution relates to the conditional probability that the difference in means is greater than zero. We can see that 43/63 subgroup relationships have $p(\Delta|data) > 0.99$.

198 same participants, will help further establish the connection between the two measurements, and
199 tease apart any additional complexity that may not have been captured by the summary statistics
200 we applied here. It has recently been demonstrated that W , a measure of perceptual goodness
201 derived from a holographic model of regularity (van der Helm and Leeuwenberg, 1996), can
202 predict EEG responses (Makin et al., 2016) and perceptual discrimination performance (Nucci
203 and Wagemans, 2007) for patterns that contain symmetry and other types of regularity. The
204 model was formulated based on dot patterns with symmetry axes centered on a single spatial
205 location. It will be important to determine if and how W can be computed for our random-noise
206 based wallpaper textures where combinations of symmetries tile the plane, and test how well it
207 can explain behavioral and brain responses to wallpapers.

208 We also find an effect of index for both our brain imaging measurements and our symmetry
209 detection thresholds. This means that the visual system not only represents the hierarchical rela-
210 tionship captured by individual subgroups, but also distinguishes between subgroups depending
211 on how many times the subgroup is repeated in the supergroup, with more repetitions leading
212 to larger pairwise differences. Our measured effect of index is relatively weak. This is perhaps
213 because the index analysis does not take into account the *type* of isometries that differentiate the
214 subgroup and supergroup. The effect of symmetry type can be observed by contrasting the mea-
215 sured SSVEP amplitudes and detection thresholds for groups *PM* and *PG* in Figure 1. The two
216 groups are comparable except *PM* contains reflection and *PG* contains glide reflection, and the
217 former clearly elicits higher amplitudes and lower thresholds. An important goal for future work
218 will be to map out how different symmetry types contribute to the representational hierarchy.

219 The correspondence between responses in the visual system and group theory that we demon-
220 strate here, may reflect a form of implicit learning that depends on the structure of the natural
221 world. The environment is itself constrained by physical forces underlying pattern formation
222 and these forces are subject to multiple symmetry constraints (Hoyle, 2006). The ordered struc-
223 ture of responses to wallpaper groups could be driven by a central tenet of neural coding, that of
224 efficiency. If coding is to be efficient, neural resources should be distributed to capture the struc-
225 ture of the environment with minimum redundancy considering the visual geometric optics, the
226 capabilities of the subsequent neural coding stages and the behavioral goals of the organism (At-
227 tneave, 1954; Barlow, 1961; Laughlin, 1981; Geisler et al., 2009). Early work within the efficient
228 coding framework suggested that natural images had a $1/f$ spectrum and that the corresponding
229 redundancy between pixels in natural images could be coded efficiently with a sparse set of ori-
230 ented filter responses, such as those present in the early visual pathway (Field, 1987; Olshausen
231 and Field, 1997). Our results suggest that the principle of efficient coding extends to a much
232 higher level of structural redundancy – that of symmetries in visual images.

233 The 17 wallpaper groups are completely regular, and relatively rare in the visual environment,
234 especially when considering distortions due to perspective and occlusion. Near-regular textures,
235 however, abound in the visual world, and can be approximated as deformed versions of the
236 wallpaper groups (Liu et al., 2004). The correspondence between visual cortex responses and
237 group theory demonstrated here may indicate that the visual system represents visual textures
238 using a similar scheme, with the wallpaper groups serving as anchor points in representational

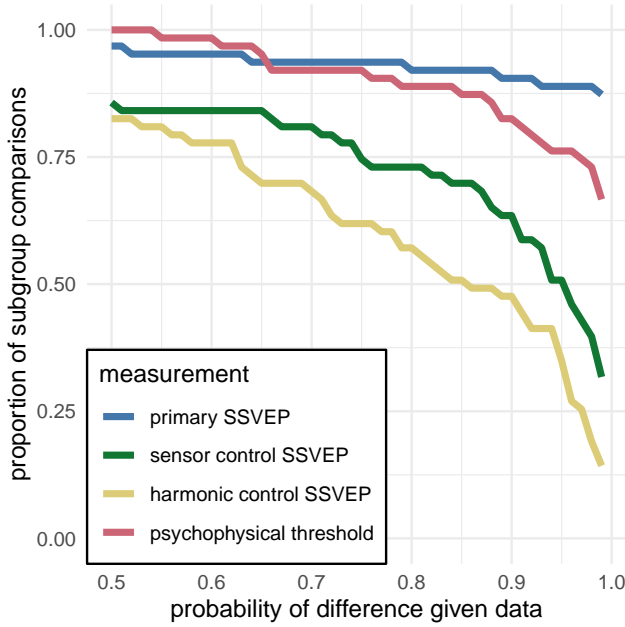


Figure 4: This plot shows the proportion of subgroup relationships that satisfy $p(\Delta > 0 | data) > x$. We can see that if we take $x = 0.95$ as our threshold, the subgroup relationships are preserved in $56/63 = 89\%$ and $49/64 = 78\%$ of the comparisons for the primary SSVEP and threshold duration datasets, respectively. This compares to the $32/64 = 50\%$ and $22/64 = 35\%$ for the SSVEP control datasets.

space. This framework resembles norm-based encoding strategies that have been proposed for other stimulus classes, most notably faces (Leopold et al., 2006), and leads to the prediction that adaptation to wallpaper patterns should distort perception of near-regular textures, similar to the aftereffects found for faces (Webster and MacLin, 1999). Field biologists have demonstrated that animals respond more strongly to exaggerated versions of a learned stimulus, referred to as “supernormal” stimuli (Tinbergen, 1953). In the norm-based encoding framework, wallpaper groups can be considered *supertextures*, exaggerated examples of the near-regular textures that surround us. Artists may consciously or unconsciously create supernormal stimuli, to capture the essence of the subject and evoke strong responses in the audience (Ramachandran and Hirstein, 1999). Wallpaper groups are visually compelling, and symmetries have been widely used in human artistic expression going back to the Neolithic age (Jablan, 2014). If wallpapers are in fact supertextures, this prevalence may be a direct result of the strategy the human visual system has adopted for texture encoding.

Participants

Twenty-five participants (11 females, mean age 28.7 ± 13.3) took part in the EEG experiment. Their informed consent was obtained before the experiment under a protocol that was approved by the Institutional Review Board of Stanford University. 11 participants (8 females, mean age 20.73 ± 1.21) took part in the psychophysics experiment. All participants had normal or corrected-to-normal vision. Their informed consent was obtained before the experiment under a protocol that was approved by the University of Essex’s Ethics Committee.

259 **Stimulus Generation**

260 Exemplars from the different wallpaper groups were generated using a modified version of the
261 methodology developed by Clarke and colleagues(Clarke et al., 2011) that we have described in de-
262 tail elsewhere(Kohler et al., 2016). Briefly, exemplar patterns for each group were generated from
263 random-noise textures, which were then repeated and transformed to cover the plane, according
264 to the symmetry axes and geometric lattice specific to each group. The use of noise textures as
265 the starting point for stimulus generation allowed the creation of an almost infinite number of
266 distinct exemplars of each wallpaper group. To make individual exemplars as similar as possible
267 we replaced the power spectrum of each exemplar with the median across exemplars within a
268 group. We then generated control exemplars that had the same power spectrum as the exemplar
269 images by randomizing the phase of each exemplar image. The phase scrambling eliminates ro-
270 tation, reflection and glide-reflection symmetries within each exemplar, but the phase-scrambled
271 images inherent the spectral periodicity arising from the periodic tiling. This means that all
272 control exemplars, regardless of which wallpaper group they are derived from, are transformed
273 into another symmetry group, namely P_1 . P_1 is the simplest of the wallpaper groups and contains
274 only translations of a region whose shape derives from the lattice. Because the different wallpaper
275 groups have different lattices, P_1 controls matched to different groups have different power spectra.
276 Our experimental design takes these differences into account by comparing the neural responses
277 evoked by each wallpaper group to responses evoked by the matched control exemplars.

278 **Stimulus Presentation**

279 Stimulus Presentation. For the EEG experiment, the stimuli were shown on a 24.5" Sony Trimas-
280 ter EL PVM-2541 organic light emitting diode (OLED) display at a screen resolution of 1920×1080
281 pixels, 8-bit color depth and a refresh rate of 60 Hz, viewed at a distance of 70 cm. The mean
282 luminance was 69.93 cd/m^2 and contrast was 95%. The diameter of the circular aperture in
283 which the wallpaper pattern appeared was 13.8° of visual angle presented against a mean lumi-
284 nance gray background. Stimulus presentation was controlled using in-house software. For the
285 psychophysics experiment, the stimuli were shown on a $48 \times 27 \text{ cm}$ VIEWPiXX/3D LCD Display
286 monitor, model VPX-VPX-2005C, resolution 1920×1080 pixels, with a viewing distance of ap-
287 proximately 40cm and linear gamma. Stimulus presentation was controlled using MatLab and
288 Psychtoolbox-3 (Kleiner et al., 2007; Brainard, 1997). The diameter of the circular aperture for
289 the stimuli was 21.5° .

290 **EEG Procedure**

291 Visual Evoked Potentials were measured using a steady-state design, in which P_1 control images
292 alternated with exemplar images from each of the 16 other wallpaper groups. Exemplar images
293 were always preceded by their matched P_1 control image. A single 0.83 Hz stimulus cycle consisted
294 of a control P_1 image followed by an exemplar image, each shown for 600 ms. A trial consisted
295 of 10 such cycles (12 sec) over which 10 different exemplar images and matched controls from
296 the same rotation group were presented. For each group type, the individual exemplar images

were always shown in the same order within the trials. Participants initiated each trial with a button-press, which allowed them to take breaks between trials. Trials from a single wallpaper group were presented in blocks of four repetitions, which were themselves repeated twice per session, and shown in random order within each session. To control fixation, the participants were instructed to fixate a small white cross in the center of display. To control vigilance, a contrast dimming task was employed. Two times per trial, an image pair was shown at reduced contrast, and the participants were instructed to press a button on a response pad. We adjusted the contrast reduction such that average accuracy for each participant was kept at 85% correct, in order to keep the difficulty of the vigilance at a constant level.

Psychophysics Procedure

The experiment consisted of 16 blocks, one for each of the wallpaper groups (excluding P_1). We used a two-interval forced choice approach. In each trial, participants were presented with two stimuli (one of which was the wallpaper group for the current block of trials, the other being P_1), one after the other (inter-stimulus interval of 700ms). After each stimulus had been presented, it was masked with white noise for 300ms. After both stimuli had been presented, participants made a response on the keyboard to indicate whether they thought the first or second image contained more symmetry. Each block started with 10 practice trials, (stimulus display duration of 500ms) to allow participants to familiarise themselves with the current block's wallpaper pattern. If they achieved an accuracy of 9/10 in these trials they progressed to the rest of the block, otherwise they carried out another set of 10 practise trials. This process was repeated until the required accuracy of 9/10 was obtained. The rest of the block consisted of four interleaved staircases (using the QUEST algorithm (Watson and Pelli, 1983), full details given in the SI) of 30 trials each. On average, a block of trials took around 10 minutes to complete.

EEG Acquisition and Preprocessing

Steady-State Visual Evoked Potentials (SSVEPs) were collected with 128-sensor HydroCell Sensor Nets (Electrical Geodesics, Eugene, OR) and were band-pass filtered from 0.3 to 50 Hz. Raw data were evaluated off line according to a sample-by-sample thresholding procedure to remove noisy sensors that were replaced by the average of the six nearest spatial neighbors. On average, less than 5% of the electrodes were substituted; these electrodes were mainly located near the forehead or the ears. The substitutions can be expected to have a negligible impact on our results, as the majority of our signal can be expected to come from electrodes over occipital, temporal and parietal cortices. After this operation, the waveforms were re-referenced to the common average of all the sensors. The data from each 12s trial were segmented into five 2.4 s long epochs (i.e., each of these epochs was exactly 2 cycles of image modulation). Epochs for which a large percentage of data samples exceeding a noise threshold (depending on the participant and ranging between 25 and 50 μ V) were excluded from the analysis on a sensor-by-sensor basis. This was typically the case for epochs containing artifacts, such as blinks or eye movements. Steady-state stimulation will drive cortical responses at specific frequencies directly tied to the stimulus frequency. It is thus appropriate to quantify these responses in terms of both phase and amplitude. Therefore, a

336 Fourier analysis was applied on every remaining epoch using a discrete Fourier transform with a
337 rectangular window. The use of two-cycle long epochs (i.e., 2.4 s) was motivated by the need to
338 have a relatively high resolution in the frequency domain, $\delta f = 0.42$ Hz. For each frequency bin,
339 the complex-valued Fourier coefficients were then averaged across all epochs within each trial.
340 Each participant did two sessions of 8 trials per condition, which resulted in a total of 16 trials
341 per condition.

342 SSVEP Analysis

343 Response waveforms were generated for each group by selective filtering in the frequency do-
344 main. For each participant, the average Fourier coefficients from the two sessions were averaged
345 over trials and sessions. The SSVEP paradigm we used allowed us to separate symmetry-related
346 responses from non-specific contrast transient responses. Previous work has demonstrated that
347 symmetry-related responses are predominantly found in the odd harmonics of the stimulus fre-
348 quency, whereas the even harmonics consist mainly of responses unrelated to symmetry, that
349 arise from the contrast change associated with the appearance of the second image (Norcia et al.,
350 2002; Kohler et al., 2016). This functional distinction of the harmonics allowed us to generate
351 a single-cycle waveform containing the response specific to symmetry, by filtering out the even
352 harmonics in the spectral domain, and then back-transforming the remaining signal, consisting
353 only of odd harmonics, into the time-domain. For our main analysis, we averaged the odd har-
354 monic single-cycle waveforms within a six-electrode region of interest (ROI) over occipital cortex
355 (electrodes 70, 74, 75, 81, 82, 83). These waveforms, averaged over participants, are shown in
356 Figure 1. The same analysis was done for the even harmonics and for the odd harmonics within a
357 six electrode ROI over parietal cortex (electrodes 53, 54, 61, 78, 79, 86; see Supplementary Figure
358 1.1). The root-mean square values of these waveforms, for each individual participant, were used
359 to determine whether each of the wallpaper subgroup relationships were preserved in the brain
360 data.

361 Defining the list of subgroup relationships

362 In order to get the complete list of subgroup relationships, we digitized Table 4 from Coxeter
363 (Coxeter and Moser, 1972) (shown in Supplementary Table 1.2). After removing identity rela-
364 tionships (i.e. each group is a subgroup of itself) and the three pairs of wallpaper groups that are
365 subgroups of each other (e.g. *PM* is a subgroup of *CM*, and *CM* is a subgroup of *PM*) we were left
366 with a total of 63 unambiguous subgroups that were included in our analysis.

367 Bayesian Analysis of SSVEP and Psychophysical data

368 Bayesian analysis was carried out using R (v3.6.1) (R Core Team, 2019) with the *brms* package
369 (v2.9.0) (Bürkner, 2017) and *rStan* (v2.19.2 (Stan Development Team, 2019)). The data from each
370 experiment were modelled using a Bayesian generalised mixed effect model with wallpaper group
371 being treated as a 16-level factor, and random effects for participant. The SSVEP data and sym-
372 metry detection threshold durations were modelled using log-normal distributions with weakly

informative, $\mathcal{N}(0, 2)$, priors. After fitting the model to the data, samples were drawn from the posterior distribution of the two datasets, for each wallpaper group. These samples were then recombined to calculate the distribution of differences for each of the 63 pairs of subgroup and supergroup. These distributions were then summarised by computing the conditional probability of obtaining a positive (negative) difference, $p(\Delta|\text{data})$. For further technical details, please see the Supplementary Materials at <https://osf.io/f3ex8/> where the full R code, model specification, prior and posterior predictive checks, and model diagnostics, can be found.

References

- Apthorp, D. and Bell, J. (2015). Symmetry is less than meets the eye. *Current Biology*, 25(7):R267–R268.
- Attneave, F. (1954). Some informational aspects of visual perception. *Psychol Rev*, 61(3):183–93.
- Barlow, H. B. (1961). *Possible principles underlying the transformations of sensory messages*, pages 217–234. MIT Press.
- Brainard, D. H. (1997). Spatial vision. *The psychophysics toolbox*, 10:433–436.
- Bürkner, P.-C. (2017). Advanced bayesian multilevel modeling with the r package brms. *arXiv preprint arXiv:1705.11123*.
- Clarke, A. D. F., Green, P. R., Halley, F., and Chantler, M. J. (2011). Similar symmetries: The role of wallpaper groups in perceptual texture similarity. *Symmetry*, 3(4):246–264.
- Cohen, E. H. and Zaidi, Q. (2013). Symmetry in text: Salience of mirror symmetry in natural patterns. *Journal of vision*, 13(6).
- Coxeter, H. S. M. and Moser, W. O. J. (1972). *Generators and relations for discrete groups*. Ergebnisse der Mathematik und ihrer Grenzgebiete ; Bd. 14. Springer-Verlag, Berlin, New York.
- Fedorov, E. (1891). Symmetry in the plane. In *Zapiski Imperatorskogo S. Peterburgskogo Mineralogicheskogo Obshchestva [Proc. S. Peterb. Mineral. Soc.]*, volume 49, pages 345–390.
- Field, D. J. (1987). Relations between the statistics of natural images and the response properties of cortical cells. *J Opt Soc Am A*, 4(12):2379–94.
- Geisler, W. S., Najemnik, J., and Ing, A. D. (2009). Optimal stimulus encoders for natural tasks. *Journal of Vision*, 9(13):17–17.
- Hoyle, R. B. (2006). *Pattern formation: an introduction to methods*. Cambridge University Press.
- Jablan, S. V. (2014). *Symmetry, Ornament and Modularity*. World Scientific Publishing Co Pte Ltd, Singapore, SINGAPORE.
- Keefe, B. D., Gouws, A. D., Sheldon, A. A., Vernon, R. J. W., Lawrence, S. J. D., McKeefry, D. J., Wade, A. R., and Morland, A. B. (2018). Emergence of symmetry selectivity in the visual areas of the human brain: fMRI responses to symmetry presented in both frontoparallel and slanted planes. *Human Brain Mapping*, 39(10):3813–3826.
- Kleiner, M., Brainard, D., Pelli, D., Ingling, A., Murray, R., and Broussard, C. (2007). What's new in psychtoolbox-3. *Perception*, 36:1–16.
- Kohler, P. J., Clarke, A., Yakovleva, A., Liu, Y., and Norcia, A. M. (2016). Representation of maximally regular textures in human visual cortex. *The Journal of Neuroscience*, 36(3):714–729.
- Kohler, P. J., Cottereau, B. R., and Norcia, A. M. (2018). Dynamics of perceptual decisions about symmetry in visual cortex. *NeuroImage*, 167(Supplement C):316–330.
- Landwehr, K. (2009). Camouflaged symmetry. *Perception*, 38:1712–1720.
- Laughlin, S. (1981). A simple coding procedure enhances a neuron's information capacity. *Z Naturforsch C*, 36(9-10):910–2.
- Leopold, D. A., Bondar, I. V., and Giese, M. A. (2006). Norm-based face encoding by single neu-

- 444 rons in the monkey inferotemporal cortex. *Nature*, 442(7102):572–5.
- 445 484 Palmer, S. E. (1985). The role of symmetry in shape perception. *Acta Psychologica*, 59(1):67–90.
- 446 Li, Y., Sawada, T., Shi, Y., Steinman, R., and Pizlo, Z. (2013). *Symmetry Is the sine qua non of Shape*, book section 2, pages 21–40. Advances in Computer Vision and Pattern Recognition. Springer London.
- 447 488 Polya, G. (1924). Xii. Über die analogie der kristallsymmetrie in der ebene. *Zeitschrift für Kristallographie-Crystalline Materials*, 60(1):278–282.
- 448 489 R Core Team (2019). *R: A Language and Environment for Statistical Computing*. R Foundation for Statistical Computing, Vienna, Austria.
- 449 490 Ramachandran, V. S. and Hirstein, W. (1999). The science of art: A neurological theory of aesthetic experience. *Journal of Consciousness Studies*, 6(6–7):15–41.
- 450 491 Liu, Y., Hel-Or, H., Kaplan, C. S., and Van Gool, L. (2010). Computational symmetry in computer vision and computer graphics. *Foundations and Trends® in Computer Graphics and Vision*, 5(1–2):1–195.
- 451 492 493
- 452 494 Liu, Y., Lin, W.-C., and Hays, J. (2004). Near-regular texture analysis and manipulation. In *ACM Transactions on Graphics (TOG)*, volume 23, pages 368–376. ACM.
- 453 495 Makin, A. D. J., Wright, D., Rampone, G., Palumbo, L., Guest, M., Sheehan, R., Cleaver, H., and Bertamini, M. (2016). An Electrophysiological Index of Perceptual Goodness. *Cerebral Cortex*, 26(12):4416–4434.
- 454 496 497
- 455 498 Møller, A. P. (1992). Female swallow preferences for symmetrical male sexual ornaments. *Nature*, 357(6375):238–240.
- 456 499 500 501 Stan Development Team (2019). RStan: the R interface to Stan. R package version 2.19.2.
- 457 502 Tinbergen, N. (1953). *The herring gull's world: a study of the social behaviour of birds*. Frederick A. Praeger, Inc., Oxford, England.
- 458 503 504
- 459 505 Norcia, A. M., Appelbaum, L. G., Ales, J. M., Cottereau, B. R., and Rossion, B. (2015). The steady-state visual evoked potential in vision research: a review. *Journal of Vision*, 15(6):4–4.
- 460 506 507 508 509
- 461 509 Norcia, A. M., Candy, T. R., Pettet, M. W., Vildavski, V. Y., and Tyler, C. W. (2002). Temporal dynamics of the human response to symmetry. *Journal of Vision*, 2(2):132–139.
- 462 510 511 512
- 463 513 Nucci, M. and Wagemans, J. (2007). Goodness of Regularity in Dot Patterns: Global Symmetry, Local Symmetry, and Their Interactions. *Perception*, 36(9):1305–1319. Publisher: SAGE Publications Ltd STM.
- 464 514 515 516 517
- 465 518 Olshausen, B. A. and Field, D. J. (1997). Sparse coding with an overcomplete basis set: a strategy employed by v1? *Vision Res*, 37(23):3311–25.
- 466 519 520 Webster, M. A. and MacLin, O. H. (1999). Figural aftereffects in the perception of faces. *Psychon Bull Rev*, 6(4):647–53.